Dysprosium Doped Dielectric Materials for Sintering in Reducing Atmospheres

WEN-HSI LEE,[1] W.A. GROEN,[2] HERBERT SCHREINEMACHER[2] & DETLEV HENNINGS[2]

[1]Philips Passive Components Kaohsiung (PPCK), Taiwan
*[2]Philips Research Laboratories, 52066 Aachen, Germany*

Abstract. Substitution of Dy rare earth ions was studied in $Ba(Ti,Zr)O_3$ dielectric materials, using thermogravimetry, X-ray diffraction and dielectric measurements. Dy^{3+} ions enter both the A- and the B-sites of the perovskite structure, however, the solubility on B-sites is up to 9 mol %, whereas it is only 2.5 mol % on A-sites. Dy can be easily shifted from A- to B-sites and back, using Ba or Ti excess in the material. Dy^{3+} on B-sites is a strong electron acceptor. Dy doped dielectric materials are cofired with Ni electrodes in reducing atmosphere to highly insulating BME multilayer capacitors.

Keywords: multilayer capacitors, base metal electrodes, rare earth acceptors, $B_a(T_i Z_r)O_3$, dielectric

1. Introduction

Recent advancements in the technology of base metal electrodes (BME) enabled the producers of ceramic multilayer capacitors (MLCCs) to replace the relatively expensive Ag-Pd inner electrodes by cheaper Ni electrodes. Because of the easy oxidizability of Ni, BME capacitors must be sintered in a protective atmosphere of moist H_2/N_2 or CO/CO_2. In reducing atmospheres the Ti^{4+} ions of $BaTiO_3$ based ceramics are partly reduced to Ti^{3+}. Large numbers of ionized oxygen vacancies and electrons are formed [1,2] which give rise to a high electronic conductivity. The change of conductivity after firing in reducing atmosphere is up to 13 orders of magnitude.

$$BaTiO_3 + x/2H_2 \longrightarrow BaTiO_{3-x}[V_O]_x$$

$$+ x/2\ H_2O$$
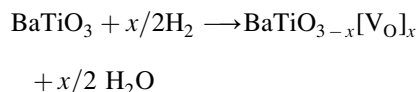
Ionization of V_O results in the formation of conduction electrons:

$$[V_O] \longrightarrow [V_O]^{\cdot\cdot} + 2e'$$

Conduction electrons formed at reducing atmosphere in the dielectric material can be readily trapped by acceptor ions in the perovskite lattice [3]. Strong electron acceptors are for instance $Ca^{2+}-$, $Mg^{2+}-$ and $Mn^{2+}-$ ions [2,3,6] on Ti-sites.

Electron conduction is suppressed by acceptor doping:

$$Ca^{2+}_{(Ti)}, Mn^{2+}_{(Ti)} + 2e' \longrightarrow [Ca^{2+}_{(Ti)}]'',$$

$$[Mn^{2+}_{(Ti)}]'', E_a \geq 2\ eV$$
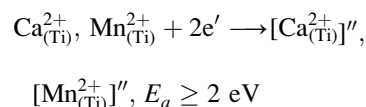
After incorporation of strong electron acceptors the dielectric materials become highly insulating [7] and can be used at temperatures up to 250°C. Even after suppression of the electron conduction a considerable ionic conduction remains in the material which gives rise to degradation of the insulation resistance (IR) under electric field and temperature stress [8]. The ion conduction results from migration of charged oxygen vacancies in the electric field [9]. Especially in thin dielectric layers of BME material electromigration of charged oxygen vacancies leads to rapid degradation. Elimination of charged oxygen vacancies is thus one of the most challenging problems of BME materials.

1.1. Improvement of Life Stability

1.1.1. Re-oxidation. Oxygen vacancies can be eliminated from BME materials in several ways. A convenient method of increasing the life stability of BME capacitors is re-oxidation of the MLCCs after firing in reducing atmosphere. At re-oxidation in weakly oxidizing atmosphere valence unstable acceptor ions change their valence states to higher values:

$$Mn^{2+} \longrightarrow Mn^{3+,4+}$$
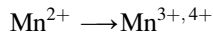
As a result of the re-oxidation, parts of the oxygen vacancies, formed to compensate the lower valence states of Mn, are eliminated, corresponding to the valence change.

$$2[Mn^{2+}_{(Ti)}]'' + 2[V_O]^{\bullet\bullet} + \frac{1}{2}O_2$$
$$\longrightarrow 2[Mn^{3+}_{(Ti)}]' + 1[V_O]^{\bullet\bullet}$$
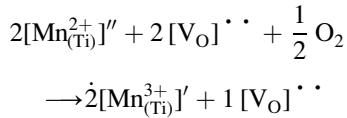
Complete elimination of the oxygen vacancies by oxidation to Mn^{4+}, however, is not possible, because the high required oxygen pressures would lead to total corrosion of the Ni inner electrodes.

1.1.2. Donor-acceptor complex formation. A considerable improvement of the life stability is observed in BME materials which have been doped with combinations of donor and acceptor ions. Donor and acceptor ions compensate each other, so that oxygen vacancies are no longer necessary. The interaction between donors and acceptors is strongly non-linear, being thus not comparable to chemical complex formation [10].

$$[Mn^{2+}_{(Ti)}]'' + 2[Nb^{5+}_{(Ti)}]^{\bullet} \longrightarrow \{[Nb^{5+}_{(Ti)}]^{\bullet}$$
$$- [Mn^{2+}_{(Ti)}]'' - [Nb^{5+}_{(Ti)}]^{\bullet}\}^0$$
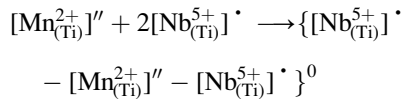
Charge complexes between Mn^{2+}- and Nb^{5+}-ions are highly stable, so that the Mn^{2+}-ions cannot be oxidized to Mn^{3+} even in air atmosphere [10,11]. Donor acceptor charge complexes are supposed to form thin inversion layers at the grain boundaries, showing donor character. The inversion layers are assumed to suppress electromigration of oxygen vacancies [12].

1.1.3. Rare earth dopes. A succesful way to improve the life stability of BME materials is the incorporation of certain rare earth (RE) dopes. Y^{3+}, Dy^{3+}, Ho^{3+} and Gd^{3+}, which are sometimes called the ''Magic Ions'' [13] exhibit a relatively small ionic radius [14] which enables them to enter both the A and the B-sites of the perovskite structure [15]. The magic RE ions are thus suspected to act as donors as well as acceptors in $BaTiO_3$. Y^{3+} and Dy^{3+} dopes are primarily known to act as donors in $BaTiO_3$, being commonly used at the manufacture of semiconducting PTCR thermistors.

This paper deals with a study of the dopant character of Dy^{3+} in $Ba(Ti,Zr)O_3$. Dy dopes are used at the production of BME MLCCs showing the dielectric temperature characteristic ''Y5V''.

2. Experimental

The incorporation of Dy in BTZ was studied by means of thermogravimetry TGA and X-ray diffraction (XRD). The lattice parameters were determined, using a Si standard at room temperature. For easier determination of the lattice constants we used cubic perovskites of the general composition $(Ba_{1-x}Dy_x)[Ti_{0.78}Zr_{0.22}]O_3$. Ceramic powders were prepared by calcination of reagent grade $BaCO_3$, TiO_2, ZrO_2 and Dy_2O_3 at 1200°C in air. The Dy content was varied between $0 \leq x \leq 0.15$. For XRD experiments three series of samples were prepared at 1200°C. The Ba-content was adjusted in the way, that one series had Dy totally on B-sites, the other one Dy totally on A-sites, and the third one Dy on both A- and B-sites. Above the neccessary amount of $BaCO_3$ or TiO_2 to fix the Dy on A- or B-sites a small excess of $BaCO_3$ or TiO_2 was added.
1. **Dy on B-sites:** $Ba[(Ti_{0.78}Zr_{0.22})_{1-x}Dy_x]O_3$, $0 \leq x \leq 0.10$, Ba-excess of 0.02 mol
2. **Dy on A- and B-sites:** $(Ba_{1-a}Dy_a)[(Ti_{0.78}Zr_{0.22})_{1-b}Dy_b]O_3$, $a+b=x$; $0 \leq x \leq 0.10$, no Ba-, no Ti-excess.
3. **Dy on A-sites:** $(Ba_{1-x}Dy_x)[Ti_{0.78}Zr_{0.22}]O_3$, $0 \leq x \leq 0.10$, Ti-excess of 0.005 mol.

For thermogravimetric experiments various amounts of $BaCO_3$ were added after calcination in order to shift the Dy^{3+} from A to B sites.

For dielectric measurements ceramic discs of the composition $Ba[(Ti_{0.82}Zr_{0.18})_{1-x}Dy_x]O_3$ ($0 \leq x \leq 0.15$), showing 5 mm diameter and 0.5 mm

thickness, were sintered at 1300°C in an atmosphere of moist N_2/H_2, which had an oxygen partial pressure of $P_{O_2} = 10^{-11}$ bar. The amount of $BaCO_3$ was adjusted in the way that all Dy^{3+} ions could enter the B-sites as electron acceptors.

3. Results

3.1. XRD Measurements

All materials prepared showed a cubic perovskite lattice. The lattice constants determined as function of the Dy concentration at 25°C, are shown in Fig. 1. The lattice constants of BDTZ with Dy completely incorporated on B- or A-sites follow simple Vegard lines. Dy^{3+} obviously exhibits a preference for the B-sites. According to the larger atomic radius [14] of Dy^{3+} ($R_{[B]} = 0.091$ nm) compared to Ti^{4+} ($R_{[B]} = 0.068$ nm), samples containing Dy on B-sites show a continuous increase of the lattice constants. The maximum solubility of Dy on B-sites is up to ca. 9 mol %. The maximum solubility of Dy^{3+} on A-sites is in contrast only 2.5 mol %. Corresponding to the smaller ionic radius of Dy^{3+} on A-sites ($R_{[A]} = 0.117$ nm) compared to Ba^{2+} ($R_{[Ba]} = 0.134$ nm), the lattice parameters of BDTZ with Dy^{3+} on A-sites show a slight decrease. The lattice parameters of BDTZ containing Dy^{3+} both on A- and B-sites are between those of the 2 Vegard lines.
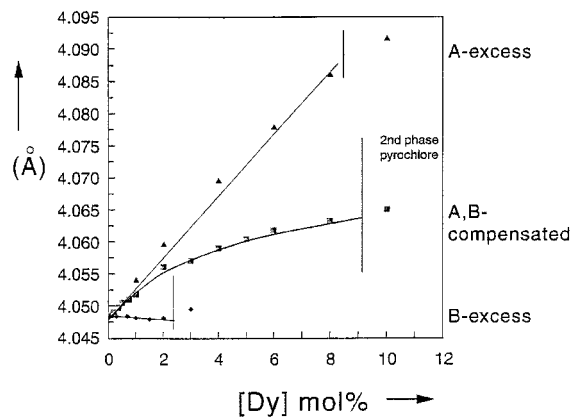
At too high Ba or Ti excess in the material the following second phases were often observed.

For too high A-excess ($BaCO_3$): Ba_{12} $Dy_{4.67}Ti_8O_{35}$

For too high B-excess (TiO_2): $Dy_2Ti_2O_7$

These phases were identified, using the ICDD File [16]. $Dy_2Ti_2O_7$ is isomorphous to $Gd_2Ti_2O_7$, thus showing a very similar XRD diagram. Dy-containig second phases were also formed in the case of not carefully mixing the raw materials. Such ''non-equilibrium'' phases were very stable and would not disappear even after long term annealing.

3.2. Application of Vegard's Law

The 2 Vegard lines of BDTZ containing Dy^{3+} on A- or B-sites were employed to calculate the amount of Dy^{3+} on A- and on B-sites for samples of Series 2. The lattice constant of BDTZ, containing Dy both on A- and B-sites is

$$a_{(A,B)} = N_A \cdot a_{(A)} + (1 - N_A) \cdot a_{(B)}$$

The molar concentrations of Dy^{3+} on A- or B-sites, determined from XRD results, have been compared to those derived from the amount of $BaCO_3$, weighed in at the preparation, always assuming that the ratio of atoms on A- and B-sites is A/B = 1. Figure 2 shows excellent agreement for the Dy concentrations, determined by the 2 different ways.

Fig. 1. Lattice constants of cubic BDTZ: (a) $Ba[(Ti_{0.78}Zr_{0.22})_{1-x}Dy_x]O_3 (0 \leq x \leq 0.10)$. Dy on B-sites, 2 mol % Ba-excess; (b) Dy on A- and B-sites: $(Ba_{1-a}Dy_a)[(Ti_{0.78}Zr_{0.22})_{1-b}Dy_b]O_3$; $a + b = x$; $0 \leq x \leq 0.10$, no Ba-, no Ti-excess; (c) $(Ba_{1-x}Dy_x)[Ti_{0.78}Zr_{0.22}]O_3$; $0 \leq x \leq 0.03$ Ti-excess of 0.005 mol.
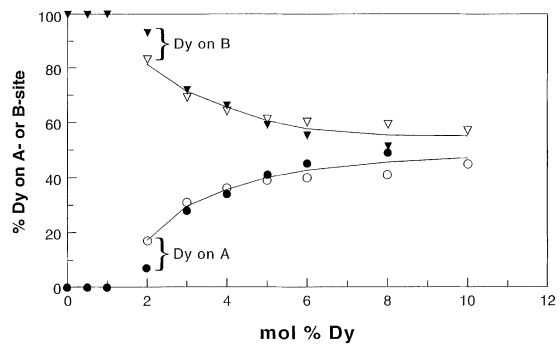

Fig. 2. Comparison of Dy site occupation in BDTZ: $(Ba_{1-a}Dy_a)[(Ti_{0.78}Zr_{0.22})_{1-b}Dy_b]O_3$; $a + b = x$; $0 \leq x \leq 0.10$. Full symbols: XRD (Vegard) determination. Open symbols: Calculated from weight of ingredients (A/B ratio).

3.3. TGA Measurements

3.3.1. The Dy-shift. At the reaction of $BaCO_3$ with BDTZ certain amounts of Dy are shifted from A- to B-sites. and CO_2 gas is evaporated which can be determined with TGA.

$$(Ba_{1-x}Dy_x)TiO_3 + 2x\, BaCO_3 \longrightarrow (Ba_{1+x})$$
$$(TiDy_x)O_{3+2x} + 2x\, CO_2 \qquad (1)$$
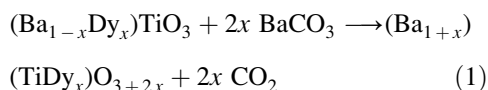
$2BaCO_3$ are needed to shift 1 Dy^{3+} from A to B. The Dy-shift, Reaction (1) was found to be irreversible at $1260°C$ in pure CO_2 atmosphere. $BaCO_3$ which is not consumed by reaction (1) decomposes to BaO, reacting to $Ba_2(Ti,Zr)O_4$

$$BaCO_3 \quad \longleftrightarrow \quad BaO + CO_2, \qquad (2)$$
$$(BaO \text{ forms } Ba_2(Ti,Zr)O_4)$$
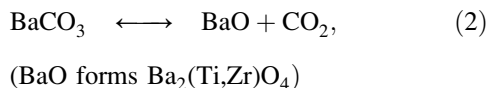
Reaction (2) is in contrast to Reaction (1) reversible in CO_2 atmosphere at $T < 1260°C$. Reaction (2) was therefore used in combination with Reaction (1) to determine exactly the amount of $BaCO_3$ required for the shift of Dy from A to B-sites. The TGA diagram, Fig. 3, shows the reversible decomposition of $BaCO_3$ which was not consumed by Reaction (1). Similar experiments were carried out earlier [17] at the shift of Ca^{2+}-ions from A to B-sites in BTZ. The TGA confirmed, that Dy^{3+} can be completely shifted from A to B sites and exactly 2 Ba were needed to shift 1 Dy from A to B sites.

3.4. Dielectric Measurements

Dielectric measurments performed at 1V ac and 1 KHz, revealed a strong shift of the Curie point (T_C) by the Dy dope to lower temperatures, see Fig. 4. The Curie point shift might be used as a suitable means to dermine the solubility of Dy in BTZ. Diffuse phase transitions at $x \geq 0.04$, however, made the determination of the maximum solubility of Dy in BTZ as function of the T_C shift impossible, see Fig. 4.

In the case of diffuse ferroelectric phase transitions the Curie-Weiss law $(1/\varepsilon = C_W/(T_C - T_{CW}))$ is only valid at temperatures far above the Curie point T_c. The Curie-Weiss temperature T_{CW} was therefore determined from the dielectric region far above T_C by extrapolating the reverse dielectric constant to zero $(1/\varepsilon \rightarrow 0)$. Figure 5 shows a continuous decrease of T_{CW} up to a Dy concentration $x \approx 0.08$. This value is in good agreement with the maximum solubility of Dy on B-sites of ≈ 9 at %, as determinined by XRD. The decrease of the Curie-Weiss temperature is $\Delta T_{CW} \approx 22.5°C/\%$ Dy

4. Discussion

Numerous papers about rare earth substitution of $BaTiO_3$ provide a contradictive picture of the lattice site occupation of Y^{3+} and Dy^{3+}. Both ions can be considered as very similar in their ionic radius, valence stability, and electronic effect in $BaTiO_3$. Furthermore both ions are commonly employed as donor dopes in $BaTiO_3$ based PTC resistors.
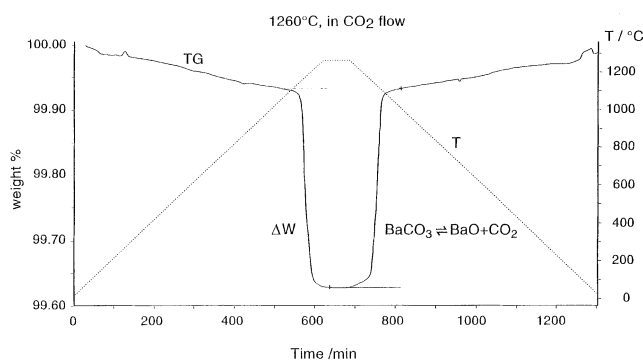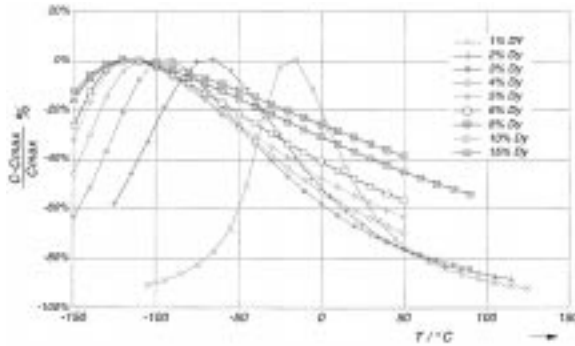

Fig. 3. Thermogravimetric analysis (TGA) of Ba-excess in BTZ-1Dy, $1260°C$, CO_2 atmosphere. Residual weight change: $\delta w(\text{expected}) = 0.31\%$; $\delta w(\text{measured}) = 0.34\%$.

Fig. 4. Dielectric temperature characteristics of Ba[(Ti$_{0.82}$-Zr$_{0.18}$)$_{1-x}$Dy$_x$]O$_3$, ($0 \leq x \leq 0.15$), measured on sintered ceramic disc capacitors at 1 KHz.

Sato et al. [18] reported strong indications for exclusive substitution of Y^{3+} on Ba-sites. Y donors would diminish the number of oxygen vacancies. Zhi et al. [19] observed a strong preference of Y for the Ti-sites and only slight solubility on A-sites. Y^{3+} acceptors would increase the number of oxygen vacancies. Buscaglia et al. [20] calculated by means of atomistic simulation an increasing tendency for Er^{3+} and Y^{3+} to substitute on Ti-sites. Hitomi et al. [21] already suspected that Y^{3+} can enter both the Ba- and Ti-sites, depending on the oxygen partial pressure. Kishi et al. [13] observed for Er^{3+}, Ho^{3+} and Dy^{3+} a prevailing trend of self-compansation between RE donors on A-sites and RE acceptors on B-sites. The present experimental investigation revealed for Dy^{3+} a strong preference to substitute on B-sites. Dy can in fact also enter the A-sites or simultaneously the A- and B-sites (self compensation). The distribution of Dy over A- and B-sites is determined by the A/B atomic ratio, i.e., by the excess of Ba or Ti in the material. However, there are also indications that the oxygen partial pressure influences the distribution of Dy over A- and B-sites.

For most of the BaTiO$_3$-based dielectric materials the A/B ratio is a highly critical parameter. Slight deviations from the stoichiometric point (A/B = 1) already lead to formation of either Ba$_2$TiO$_4$ or Ba$_6$Ti$_{17}$O$_{40}$ second phase. Small alternations of the A/B ratio thus decide on severe changes of the sintering behavior, the grain size and dielectric properties. Addition of amphoteric Dy^{3+}-ions, however, results in a broadening of the monophasic region around the stoichiometric point. Dy dopes widen the processing window of BaTiO$_3$ based dielectric materials. Slight deviations of the prescribed Ba or Ti content thus have minor influence on the electrical properties.

Acknowledgment
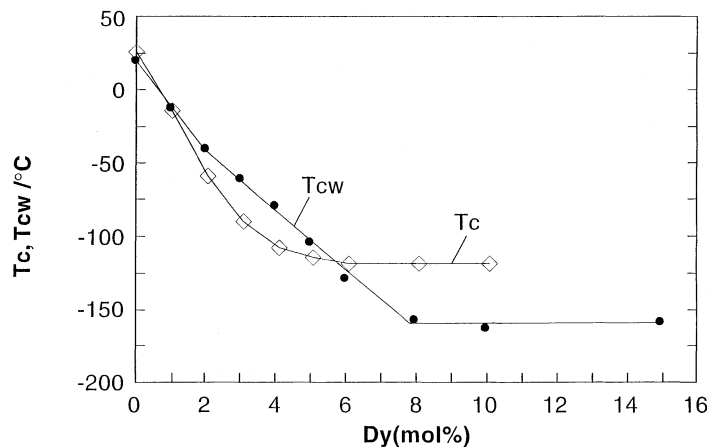
Fig. 5. Curie point (T_C) and Curie-Weiss temperature T_{CW} of Ba[(Ti$_{0.82}$Zr$_{0.18}$)$_{1-x}$Dy$_x$]O$_3$ as function of the Dy-concentration x.

References

1. J. Daniels, K.-H. Härdtl, D. Hennings, and R. Wernicke, *Philips Research Reports*, **31**, 487 (1976).
2. N.H. Chan and D.M. Smyth, *J Am. Ceram. Soc.*, **67**, 285 (1984).
3. H.-J. Hagemann and D. Hennings, *J. Am. Ceram. Soc.*, **64**, 590 (1981).
4. Y. Ho Han, J.B. Appleby, and D.M. Smyth, *J. Am. Ceram. Soc.*, **70**, 96 (1987).
5. D. Hennings and H. Schreinemacher, *J. Eur. Ceram. Soc.*, **15**, 795 (1995).
6. P. Hansen, D. Hennings, and H. Schreinemacher, *J. Electroceramics*, **2:2**, 85 (1998).
7. I. Burn and G. Maher, *J. Mater. Science*, **10**, 633.
8. R. Waser, T. Baiatu, and K.-H. Härdtl, *J. Am. Ceram. Soc.*, **73**, 1645 (1990).
9. R. Waser, T. Baiatu, and K.-H. Härdtl, *J. Am. Ceram. Soc.*, **73**, 1654 (1990).
10. K. Albertsen, D. Hennings, and O. Steigelmann, *J. Electroceramics*, **2:3**, 193 (1998).
11. D. Hennings, K. Albertsen, P. Hansen, and O. Steigelmann, *Multilayer Electronic Ceramic Devices, Ceramic Transactions* Vol. **97**, edited by Jau-Ho Jean, T.K. Gupta, K.M. Nair, and K. Niwa. The Am. Ceram. Soc. (Westerville OH 1999).
12. M. Vollmann, R. Hagenbeck, and R. Waser, *J. Am. Ceram. Soc.*, **80**, 2301 (1997).
13. H. Kishi, *Proceedings of the 7th. U.S. Japan Seminar on Dielectric and Piezoelectric Ceramics*, p. 255 (1995).
14. R.D. Shannon, *Acta Cryst.*, **A32**, 751 (1976).
15. K. Takada, E. Chang, and D.M. Smyth, ''Rare Earth Additions to BaTiO$_3$,'' pp. 147–51. In *Advances in Ceramics Vol.* **19**, Multilayer Devices. Edited by by J. Blum and W.R. Cannon. Am. Ceram. Soc. (Westerville OH 1987).
16. International Center for Diffraction Data (ICDD), Newton Square, PA 19073-3273, USA (1998).
17. D. Hennings and H. Schreinemacher, *J. Eur. Ceram. Soc.*, **15**, 795–800 (1995).
18. S. Sato, Y. Nakano, A. Sato, and T. Nomura, *Jpn. J. Appl. Phys.*, **36**, 6016 (1997).
19. J. Zhi, A. Chen, Y. Zhu, P.M. Vilarinho, and J.L. Baptista, *J. Am. Ceram. Soc.*, **82**, 1345 (1999).
20. M.T. Buscaglia, M. Viviani, P. Nanni, and V. Buscaglia, Atomistic simulation study of dopant substitution in BaTiO$_3$, paper presented at the 101th Annual Meeting of the Am. Ceram. Soc., paper SB-025-99, Indianapolis 25–28th April 1999.
21. A. Hitomi, X. Liu, T.R. Shrout, and C.A. Randall, *The eighth US-Japan Seminar on Dielectrics and Piezoelectrics*, Oct. 15–18, 1997 Plymouth, MA, USA.